

# Fluid Structure Interaction Modelling of A Novel 10MW Vertical-Axis Wind Turbine Rotor Based on Computational Fluid Dynamics and Finite Element Analysis

Lin Wang<sup>1\*</sup>, Athanasios Kolios<sup>1</sup>, Pierre-Luc Delafin<sup>1</sup>, Takafumi Nishino<sup>1</sup>, Theodore Bird<sup>2</sup>

<sup>1</sup>Centre for Offshore Renewable Energy Engineering, School of Energy, Environment and Agrifood, Cranfield University, Cranfield, MK43 0AL, UK

<sup>2</sup>Aerogenerator Project Limited, Ballingdon Mill, Sudbury, CO10 7EZ, UK

## 1. Introduction

Deployment of offshore wind farms over the past decade has highlighted several difficulties associated with conventional wind turbines. Conventional HAWTs (horizontal-axis wind turbines) place their main components (such as the rotor and generator) at the top of very tall towers, making both installation and maintenance difficult and limiting their size. VAWTs (vertical-axis wind turbines) can overcome the above drawbacks by locating their main components at the base of the tower, offering easy installation and maintenance. However, the conventional VAWTs based on the Darriues concept experience a large overturning moment, resulting in heavy drive train components.

In order to lower the overturning moment, a novel 10MW VAWT (as illustrated in Fig.1) is proposed in the NOVA (Novel Offshore Vertical Axis) project [1]. In this design, a low value of overturning moment is achieved with the aid of the sails attached to the V-shape arms. Specifically, the aerodynamic loads on the sails will result in an overturning moment which counteracts the overturning moment produced by the motion of the wind on the V-shape arms, resulting in a low value of overall overturning moment on the rotor.



Figure 1. Artist concept of NOVA 10MW VAWT [1]

---

\* Presenting author. Tel.: +44(0)1234754706; E-mail address: [lin.wang@cranfield.ac.uk](mailto:lin.wang@cranfield.ac.uk)

Large wind turbines are commonly required to be designed to meet international safety standard IEC 61400-1 [2]. According to IEC 61400-1, aeroelastic effects, which are caused by FSI (fluid structure interaction), should be taken into account in the design of the turbine. Therefore, FSI modelling of wind turbine rotors has become an important part in the development of large wind turbines.

In this work, an FSI model for VAWT rotors at full scale is established. The aerodynamic loads are obtained using CFD (computational fluid dynamics) and the rotor structural responses are determined using FEA (finite element analysis). The coupling strategy of the FSI modelling is based on the one-way coupling, in which aerodynamic loads obtained from CFD are mapped to FEA. The established FSI model is applied to the simulation of the NOVA 10MW VAWT rotor in a parked condition, under a 50-year extreme wind condition. .

## 2. Approach

### 2.1. Wind turbine rotor model

The wind turbine rotor model used in this study is the NOVA 10MW VAWT rotor [1], of which the schematic is shown in Fig. 2.

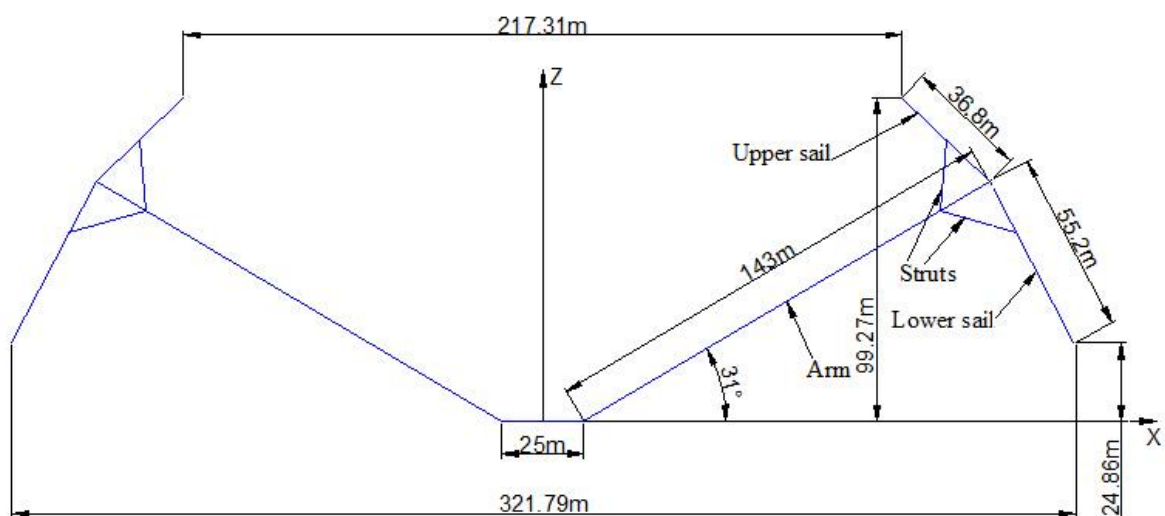


Figure 2. Schematic of NOVA 10MW VAWT rotor

The aerodynamic shape of the NOVA 10MW VAWT rotor consists of four different airfoil shapes, i.e. NACA0012, NACA0015, NACA0018 and NACA0025, as shown in Table 1. In this study, for the sake of simplicity, the struts (see Fig. 2) are ignored and the hub is regarded as a simple cuboid. The 3D geometry model of the rotor is illustrated in Fig. 3.

Table 1. Aerodynamic shape of NOVA 10MW VAWT rotor

	Chord (m)	Root profile	Tip profile
Arm	8	NACA0025	NACA0018
Upper sail	11	NACA0015	NACA0012
Lower sail	11	NACA0015	NACA0012

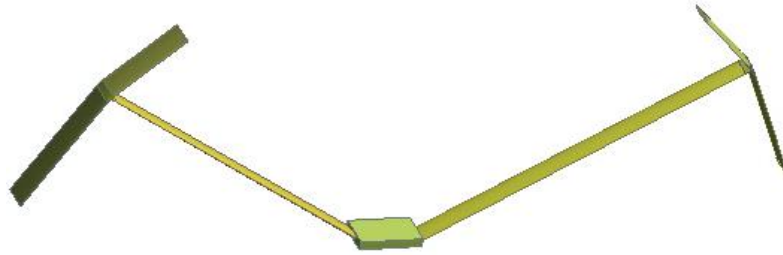


Figure 3. 3D geometry model of NOVA 10MW VAWT rotor

## 2.2. CFD modelling

### 2.2.1. Computational domain and boundary conditions

Figure 4 presents the computational domain and boundary conditions. As can be seen from Fig. 4, the rotor is contained in a large parallelepiped domain with length of  $6R$ , width of  $6R$  and height of  $3R$ , where  $R$  is the rotor radius. The rotor is regarded as a stationary non-slip wall. The velocity inlet boundary is  $1.5R$  in front of the rotor plane, the pressure outlet boundary is  $1.5R$  behind the rotor plane, and the bottom boundary is  $0.625R$  beneath the rotor. All other far-field surfaces are considered to be stationary non-slip walls. The inlet wind velocity and outlet pressure are equal to the uniform free-stream wind velocity and standard atmospheric pressure, respectively. In this study, the rotor is parked, and therefore a stationary frame is applied to the whole computational domain.

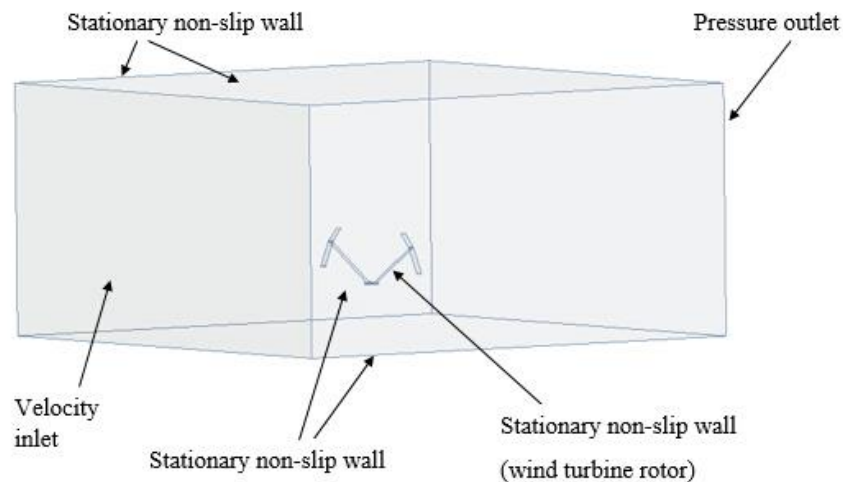


Figure 4. Computational domain and boundary conditions for CFD modelling



### 2.2.2. CFD mesh

Figs. 5 and 6 present the mesh of the whole computational domain and a section view of the mesh around the rotor, respectively. Fig. 7 shows a close view of the mesh near the rotor. As can be seen from Fig. 7, prism layers are applied to the rotor surfaces in order to have a better resolution of boundary layer flow. The element sizes of rotor surfaces and of the far-field boundary surfaces are 0.45m and 5m, respectively. The total cell number of the computational domain is approximately 2.7 million.

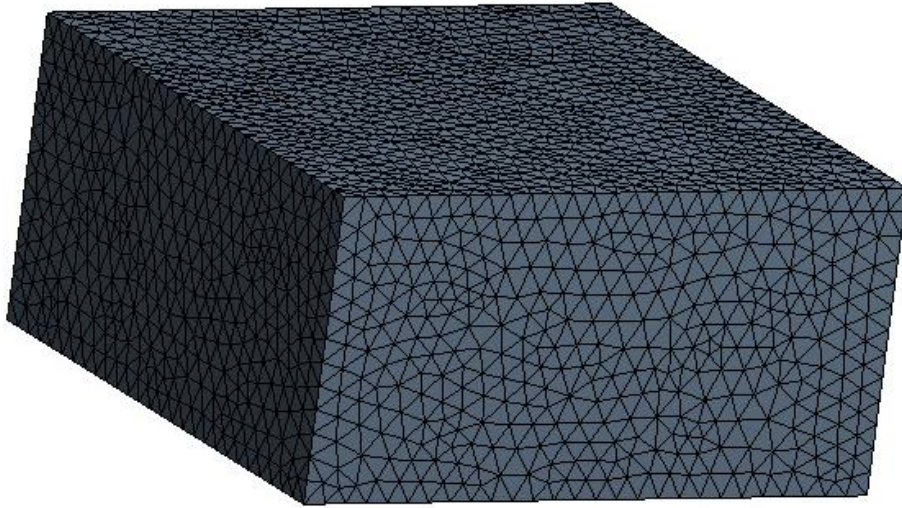


Figure 5. Mesh of the whole computational domain



Figure 6. Section view of the mesh around the rotor

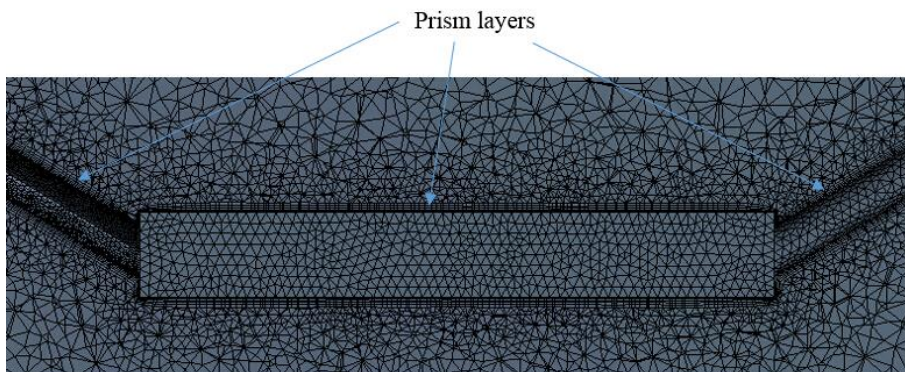


Figure 7. A close view of the mesh near the rotor

## 2.2.4. Turbulence model and solution methods

The turbulence model used in this study is the SST (shear-stress transport)  $k - \omega$  model [3], which has been widely used for CFD modelling of wind turbine rotors.

In this study, the RANS (Reynolds-Averaged Navier-Stokes) equations are solved using the pressure-based coupled algorithm [4], in which the momentum equations and the pressure-based continuity equation are solved in a closely coupled way.

## 2.3. FEA modelling

### 2.3.1. Material properties and thickness distributions

The detailed structural data of the NOVA 10MW VAWT rotor, such as composite layups, shear web locations and material properties, are not publicly available. For this reason, the rotor structure in this study is simply assumed to be made of a single composite material and the shear webs are ignored. The material properties of the rotor used in this study are shown in Table 2. The thickness distributions of the rotor blade (arm and sails) are assumed to linearly increase from the tip to the root, as illustrated in Fig. 8.

Table 2. Material properties of the rotor

$E_x$ (GPa)	$E_y$ (GPa)	$G_{xy}$ (GPa)	$\nu_{xy}$	$\rho$ (kg/m <sup>3</sup> )
123.00	8.20	4.71	0.31	1470.00

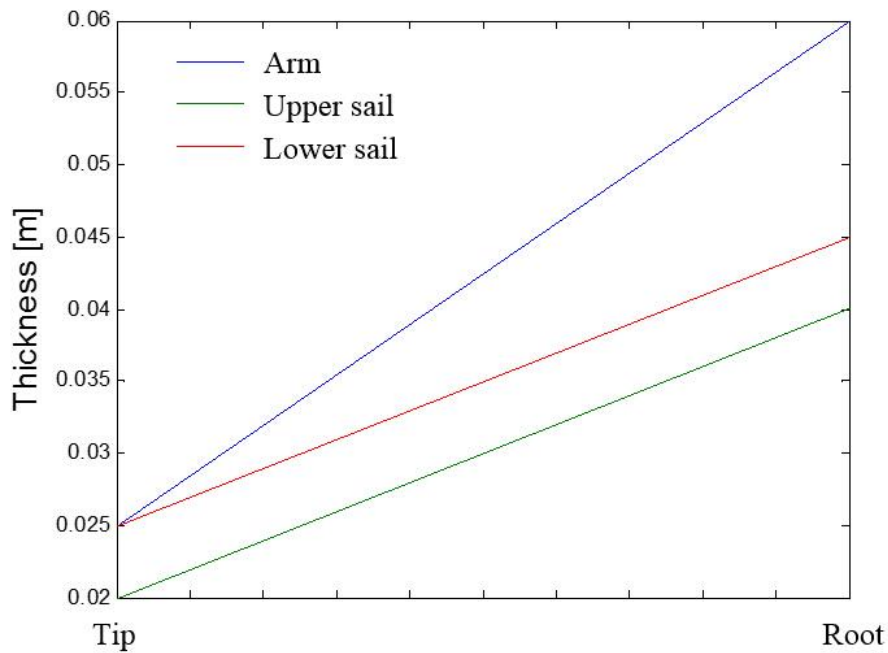


Figure 8. Thickness distribution of the rotor blade

### 2.3.2. FEA mesh and fixed boundary condition

Fig.9 presents the mesh of the rotor structure, which is meshed using structure-dominated mesh with shell elements. A close view of the mesh is shown in Fig. 10. The mesh size is 0.5m, and the total number of shell elements is 40,153.



Figure 9. Mesh of the rotor structure

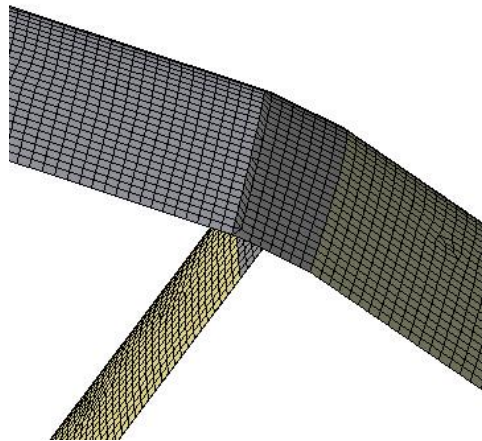


Figure 10. Close view of the mesh of the rotor structure

In this study, a fixed boundary condition is applied to the bottom surface of the hub.

### 2.4. One-way FSI coupling

In this study, the coupling strategy of the FSI modelling is based on the one-way coupling, in which the aerodynamic loads obtained from the CFD modelling are mapped to the FEA modelling. The schematic of the one-way FSI modelling is shown in Fig. 11.

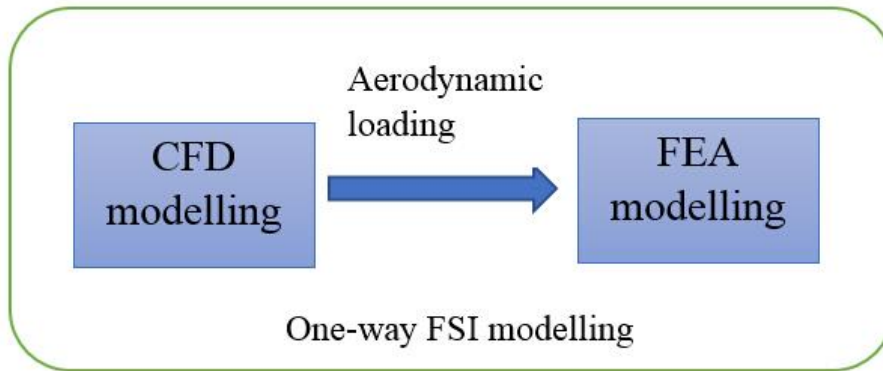


Figure 11. Schematic of one-way FSI modelling

### 3. Results and discussions

Based upon the one-way FSI modelling, the pressure distributions, deformations and stress distributions of the NOVA 10MW VAWT rotor are examined. In this case, the wind speed and rotor rotational speed are 70m/s and 0rpm, respectively. The pressure distributions on the rotor are presented in Fig. 12. Figs. 13 and 14 depict the rotor deformation and normal stress distributions, respectively.

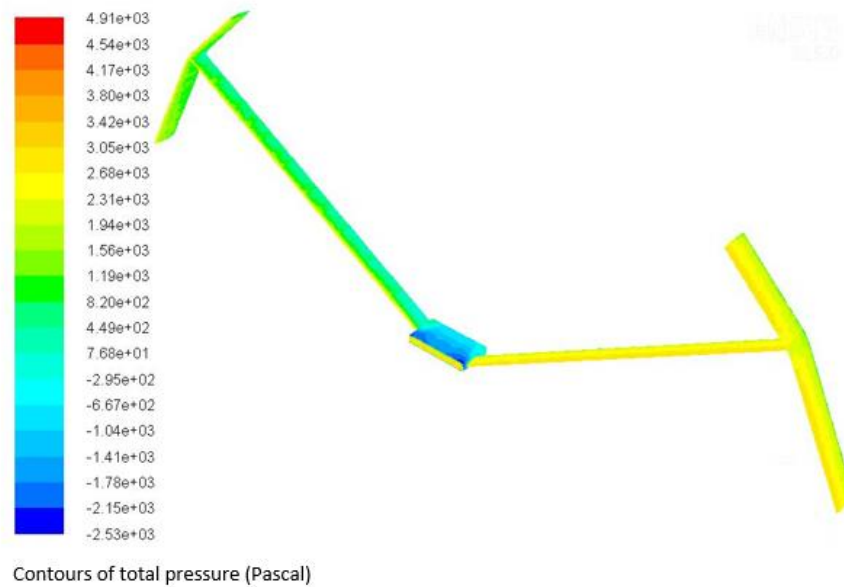


Figure 12. Rotor pressure distributions



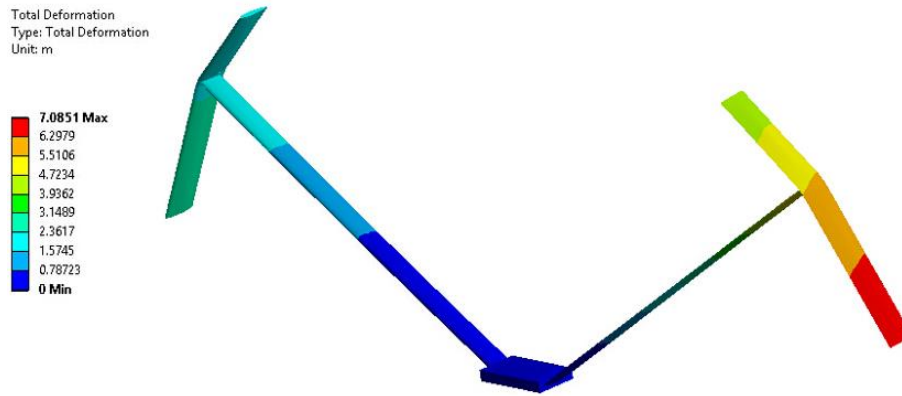


Figure 13. Rotor deformation



Figure 14. Rotor normal stress distributions

As can be seen from Fig. 12, the pressure in front of the rotor is higher than the pressure behind the rotor, producing thrust forces on the rotor. From Fig. 13 we can see that the maximum rotor deformation is approximately 7.09m, observing at the lower sail tip. As can be seen from Fig. 14, the maximum tension stress (positive normal stress) and maximum compression stress (negative normal stress) are 355.84MPa and 423.51MPa, respectively, which are within the allowable stresses.

## 4. Conclusion

In this study, an FSI (fluid structure interaction) model for VAWT (vertical-axis wind turbine) blades has been developed by coupling CFD (computational fluid dynamics) and FEA (finite element analysis). The coupling method is based on a one-way coupling, in which the aerodynamic loads obtained from CFD modelling are mapped to FEA modelling. The FSI model has been applied to the NOVA 10MW VAWT rotor, a novel large-scale VAWT rotor. The pressure distributions, blade stress distributions and blade deformations of the NOVA 10MW VAWT rotor in a parked condition, under a 50-year extreme wind condition (70m/s), have been examined based on the one-way FSI modelling.



## 5. Learning objectives

In this work, the following learning objectives have been achieved:

- To establish both CFD and FEA models of VAWT rotors
- To establish a one-way FSI model of VAWT rotors through one-way coupling of CFD and FEA
- To apply the established one-way FSI model to the simulation of the NOVA 10MW VAWT rotor in a parked condition, under a 50-year extreme wind condition

## 6. Acknowledgements

Funded by Aerogenerator Project Limited with the support of the UK Government's Department of Energy & Climate Change.

## References

- [1] D. J. Parsons, J. C. Chatterton, F. P. Brennan, and A. J. Kolios, "Carbon Brainprint Case Study: novel offshore vertical axis wind turbines," Cranfield University, 2011.
- [2] I. E. Commission, "Wind Turbines-Part 1: Design Requirements," IEC-61400-12007.
- [3] F. R. Menter, "Two-equation eddy-viscosity turbulence models for engineering applications," *AIAA journal*, vol. 32, pp. 1598-1605, 1994.
- [4] A. Fluent, "Ansys fluent 15.0 theory guide," *Ansys Inc*, 2013.